Article

Controlling the Diameter of Carbon Nanotubes in Chemical Vapor Deposition Method by Carbon Feeding

Chenguang Lu, and Jie Liu

J. Phys. Chem. B, **2006**, 110 (41), 20254-20257 • DOI: 10.1021/jp0632283

Controlling the Diameter of Carbon Nanotubes in Chemical Vapor Deposition Method by Carbon Feeding

Chenguang Lu and Jie Liu*

Department of Chemistry, Duke University, Durham, North Carolina 27708

Received: May 25, 2006; In Final Form: July 31, 2006

It was found that the diameter distribution of single-walled carbon nanotubes (SWNTs) grown by the chemical vapor deposition (CVD) method could be controlled by the carbon feeding rate at the growth stage. A unified hypothesis on the relationship between nanoparticle size, growth condition, growth temperature, and diameter of the resulting nanotubes was developed and used to explain the relationship. It was shown that the diameters of SWNTs can be controlled even when highly polydisperse nanoparticles were used as catalyst. Such control enabled us to synthesize uniform small-diameter SWNTs at low carbon feeding rates. Additionally, understanding of the important role of the carbon feeding rate can be used to explain the cause of low growth efficiency in most CVD processes. It would also help us to design methods to improve the growth efficiency of CVD growth of nanotubes.

Chemical vapor deposition (CVD), which offers versatile control and the possibility of scaling-up, is the most promising method of producing single-walled carbon nanotubes.[1−6] Many efforts[7−13] have been made toward unveiling the mechanism of SWNT growth in CVD process in order to produce SWNTs with high productivity and desired atomic structures. The unique properties of single-walled nanotubes are closely linked to their structural parameters. The diameter of the nanotubes is one such parameter that can determine the energy gap of the semiconducting nanotubes and modulate the interaction between the nanotubes and adsorbed molecules.[14] Precise control of the diameter of produced nanotubes is therefore a goal of current research. In a CVD process, most times one catalytic seed nucleates one SWNT; therefore the diameter of the SWNT is closely related to the size of its nucleating particle. On the basis of that model, researchers have been able to controllably grow SWNTs with narrow diameter distributions by using narrowly distributed[7,15−21] or identical nanoparticles[22] for CVD growth of SWNTs. However, it is often found that large portions of particles were not nucleating nanotubes, as shown in Figure 1. The growth efficiency of nanoparticles is often very low. Additionally, it was discovered that relatively uniform nanotubes can be prepared from polydisperse catalyst nanoparticles[23,24] and that the diameter of the nanotubes varies significantly as a function of the growth temperature.[20,25−28] These results painted a more complex picture than the simple idea that the diameter of the nanotubes grown is determined by the size of starting nanoparticles. Summarizing the published results and the observed relationship between various growth conditions and the diameter of the produced nanotubes, we have proposed that there exists a unified theory on the relationship between nanoparticle size, growth condition, growth temperature, and diameter of the resulting nanotubes. The key parameter for the proposed relationship is the carbon feeding rate at the growth step in a CVD process. In this paper, we have designed and performed a series of experiments to demonstrate such a proposed mechanism on diameter control. In these experiments, the carbon feeding rate is controlled by systematically varying the concentration of ethane in the feeding gas while keeping all other experimental parameters, such as growth temperature, catalyst sizes, growth time, total feeding gas flow rate, etc., unchanged. We have shown that the diameters of SWNTs can be controlled by controlling the carbon feeding rate even when highly polydisperse nanoparticles are used as catalysts. Such control enables us to synthesis uniform small-diameter SWNTs at low carbon feeding rates. Additionally, understanding of the important role of the carbon feeding rate can be used to explain the cause of the low growth efficiency in most CVD processes. It would also help us to design methods to improve the growth efficiency of the CVD growth of nanotubes.

The growth of SWNTs was performed in a 1-in. quartz tube (Technical Glass Products, Inc.) and a Lindberg/Blue M tube furnace (TF55035A). Nanoparticles were loaded on a Si wafer with 1000 nm thermal oxide coating. To achieve a wide diameter distribution of the nanoparticles, the wafer was immersed in 5 μg/g ferric nitrate in 2-propanol solution followed by a hexane rinse and blow-drying. The wafer was then annealed in air at 700 °C for 1 h to allow the formation of metal oxide nanoparticles. Figure 1a is an AFM image of the wafer surface ready for growth. Since nanoparticles may change under a given growth condition, we believe the size distribution of nanoparticles exposed to the growth condition is relevant. A loaded wafer was treated at the growth condition with 4200 ppm ethane flow at 900 °C for 1 min. Then the wafer is heated in air at 700 °C for 15 min to remove all carbon species. The AFM images showed that the nanoparticles on the substrate had a very broad diameter distribution as shown in Figure 1c. For nanotube growth, the procedure is the following: the growth chamber was sealed and vacuumed twice, followed by refilling of Ar to remove oxygen and water residue completely, since oxygen and water are known to perturb the growth of nanotubes.[29] The gas flow started with 300 sccm H_2 plus 300 sccm Ar as the temperature ramped from room temperature to the growth temperature. After the growth temperature was reached, a measured amount of Ar-diluted ethane was added into the feeding gas and the total flow rate was fixed at 1600 sccm with 56% hydrogen. The growth lasted for 5 min. Then the carbon feeding was cut off and product was protected by 300 sccm H_2

10.1021/jp0632283 CCC: $33.50
Published on Web 09/08/2006

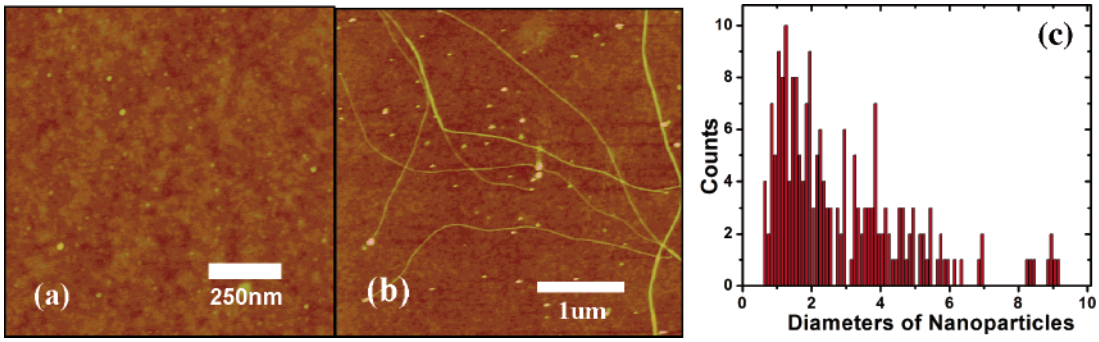

Figure 1. (a) AFM image of the surface before CVD growth shows nanoparticles of various diameters. (b) AFM image of surface after CVD growth shows SWNTs and many nonactive nanoparticles. (c) Diameter distribution of nanoparticles after 1 min ethane exposure. Nanoparticles with diameter between 1.0 and 2.0 nm are about 35% of all nanoparticles.

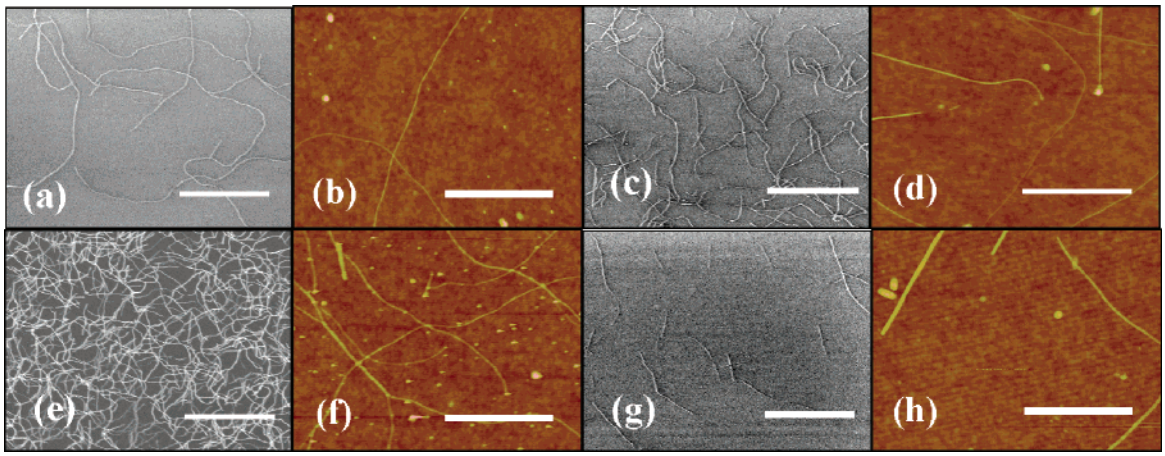

Figure 2. SEM and AFM images of SWNTs grown at different ethane concentrations. (a, b), 140 ppm; (c, d), 1600 ppm; (e, f), 4200 ppm; (g, h), 14 400 ppm. Left image in each pair, SEM image with 10 μm bar; right image in each pair, AFM image with 1 μm bar.

plus 300 sccm Ar during the cooling step. Dozens of runs were performed to map out the growth window, and only typical results were presented. Ethane was used as the carbon feeding source because its chemical activity allows the study of both high and low carbon feeding rates in the temperature range being studied (between 800 and 900 °C). Diameter data for SWNTs were taken by Raman and atomic force microscopy (AFM, from DI Instruments) in tapping mode, and the samples were also imaged with a scanning electron microscope (SEM, from FEI Company). Chemicals were used as received from Sigma−Aldrich, and gases were supplied by National Welders.

SWNTs were obtained at different carbon feeding rates at 900 °C as shown in Figure 2. Under the growth conditions described above, the concentration of ethane for effective growth of nanotubes was found to be from 10^2 to 10^4 ppm. Ethane concentration lower than 10^2 ppm and higher than 10^4 ppm yielded very few SWNTs. The growth efficiency increased at first with increasing ethane concentration and peaked at around 4200 ppm, then dropped with further increases of ethane concentration. Surfaces after growth with ethane concentration higher than 14 400 ppm were very dirty, indicating severe carbon deposition. The yield of SWNTs from nanoparticles is estimated to be 20−30% at 4200 ppm by comparing numbers of SWNTs in SEM images and nanoparticle density obtained by AFM images. A general trend in SWNT diameter, according to the AFM images in Figure 2, is that the diameters monotonically increase as ethane concentration increases, which is significant when the nanotubes grown at 14 400 and 140 ppm ethane are directly compared. Figure 3 compiles the SWNT diameter distributions of three growth conditions, and the Gaussian function is used to fit the distributions. Only features longer than 100 nm were counted. All features are weighted the same regardless of their lengths. SWNTs forming Y-junctions are considered as bundles and tracked down to their ends to find individual SWNTs before diameter values are taken. Bundles are not often seen (less than 5%) in our samples. Unfortunately, diameter distribution under the growth condition with highest yield (4200 ppm) cannot be obtained due to extensive bundle formation. Importantly, no two or more SWNTs were found to emanate from one nanoparticle. This suggests that one nanoparticle, if it is active, nucleates one and only one SWNT.

As the carbon feeding increased from 140 to 1600 ppm and then to 14 400 ppm (Figure 3), the means of the diameter distributions of SWNTs were 0.93, 1.07, and 1.78 nm and the standard deviations were 0.18, 1.12, and 1.02 nm, respectively. Raman spectroscopy also confirmed the diameter changes observed by AFM (see Supporting Information). Importantly, the Raman results proved that SWNTs dominated in our growth conditions, because we never saw broad radial breathing modes (RBM) as observed by Helmlinger et al.[30] and Endo et al.,[31] proving the existence of double-walled carbon nanotubes (DWNTs). In our Raman results, for each laser spot, the RBM peaks mostly represented carbon shells of diameters within 0.8 nm, which limited the tube type to SWNT. The diameter difference between spots is larger than this value and is consistent with the diameter distribution shown in Figure 3. Also noticeably, under 140 ppm ethane, diameters were narrowly distributed around the mean, which is unexpected and will be discussed later.

Temperature is another important factor that can change the carbon feeding rate in a CVD process. At low temperature, the

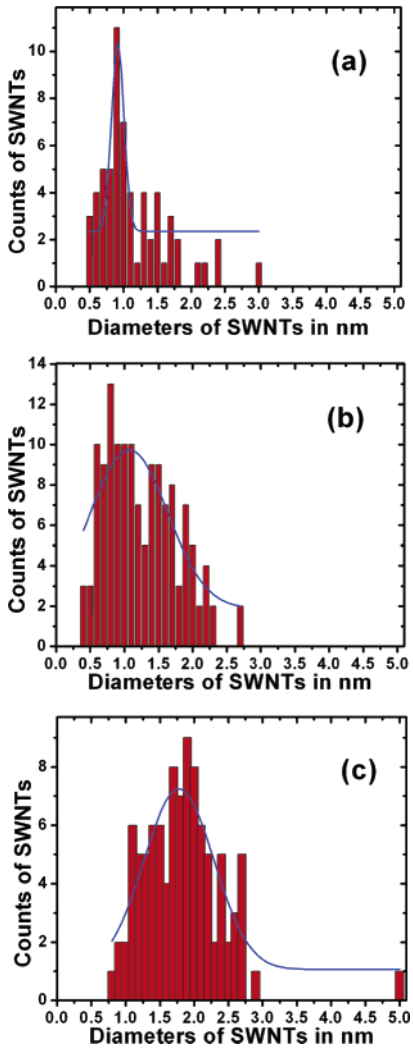

Figure 3. Diameter distributions of SWNTs grown at different ethane concentrations at 900 °C: (a) 140 ppm; (b) 1600 ppm; (c) 14 400 ppm. Curves are Gaussian fits. Means are 0.91, 1.07, and 1.78 nm and standard deviations are 0.18, 1.12, and 1.02 nm, respectively. Data are taken from height measurement of AFM images.

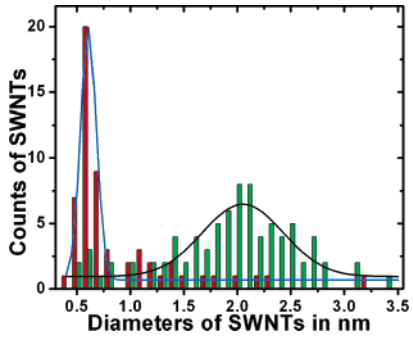

Figure 4. Diameter distributions of SWNTs grown at different ethane concentrations at 800 °C: red, 4200 ppm; green, 14 400 ppm. Curves are Gaussian fits. Means are 0.61 and 2.05 nm, and standard deviations are 0.15 and 0.76 nm, respectively. Data are taken from height measurement of AFM images. The origin of the *x*-axis is 0.3 nm.

carbon feeding rate is reduced due to slower decomposition rate of ethane. To explore the effect of temperature, systematic studies were also performed at 800 °C. Again, diameters were found to be related to ethane concentrations as shown in Figure 4. However, the effective growth window was much narrower, from 4×10^3 ppm (red bars) to 10^4 ppm (green bars). The increased lower threshold of the growth window can be

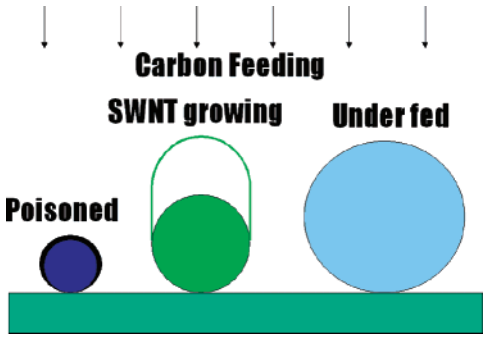

Figure 5. Activation of nanoparticles is determined by their diameters under a given carbon feeding rate. Larger particles are underfed and not nucleating growth, while smaller particles are cutoff from carbon supplies by one or more layers of graphene sheet (the black layer in this figure). Only particles with a moderate and suitable size can nucleate growth.

explained by noticing that the carbon feeding rate is reduced due to a slower decomposition rate of the precursors. Previous reports on temperature-dependent changes of SWNT diameter[20,25,26,28] should have a similar origin as discussed here. However, the fact that the growth at 800 and 900 °C possesses similar higher growth window thresholds cannot be explained by a simple explanation and could be due to the complex effects from the lowered activities of both nanoparticles and feeding gases at 800 °C in comparison with those at 900 °C.

The results discussed above clearly showed that the variation of carbon feeding rate could systematically change the diameter distribution of the nanotubes grown. Based on these results, a hypothesis on conditioned activation of nanoparticles was proposed: at any given growth condition, where the carbon feeding is fixed, there is an optimal diameter of nanoparticles to nucleate SWNTs. The larger the difference between the size of any given nanoparticle and this optimal size, the less likely such a nanoparticle will nucleate a SWNT. Smaller nanoparticles are poisoned due to "overfeeding" and larger nanoparticles are inactive due to "underfeeding" (Figure 5). In the overfeeding situation, nanoparticles smaller than the optimal size tend to be overwhelmed by excessive carbon feeding and a graphite shell would form to prevent SWNT nucleation, that is, poisoning. This deactivation of small nanoparticles was confirmed by the observation that no small-diameter SWNTs were obtained when carbon feeding reached 10 000 ppm. However, the underfeeding situation is not that well understood. From the experimental observation, larger nanoparticles did not nucleate SWNTs at low carbon feeding in the 5-min growths (140 ppm at 900 °C and 4200 ppm at 800 °C). Even after the growth time was prolonged to allow the larger particles to collect more carbon, there was still no obvious increase in total growth efficiency (see Supporting Information). That suggests that, at 800−900 °C, the larger nanoparticles lost their activities to nucleate SWNTs while waiting for an exceedingly long time to collect more carbon. For further study on this topic, we suggest in situ transmission electron microscopy monitoring changes of the nanoparticles during SWNT growth.

Since carbon feeding rate can be altered by many other experimental factors such as temperature and type of feeding gas, this hypothesis can also explain the diameter dependence on temperature[20,25−28] and the efficiency variation as shown in Figure 2. For the temperature dependence, it can be understood as the lowering of carbon feeding rate at lower temperature, resulting in smaller nanotubes at lower temperature as observed by many groups. For the observed change in growth efficiency, it can be explained as the matching of the growth conditions

with the size distribution of the specific catalyst used in our experiments, which possesses an inherent diameter distribution peaked at around 1.0−2.0 nm (Figure 1c). At the lower end of the growth window, only small particles are active and larger ones are not; hence the growth efficiency is low. After the carbon feeding rate increases, growth efficiency increases because larger particles are activated and the carbon feeding rate is not high enough to poison all the small particles. The efficiency peaks at 4200 ppm, where the carbon feeding rate is believed to favor the growth of the most populated nanoparticles in our sample. As stated earlier, under this growth condition, about 20−30% of all nanoparticles nucleate growths. According to data composing Figure 1c, the nanoparticles with diameters between 1.0 and 2.0 nm comprise about 35% of all nanoparticles. This suggests an estimated 57−86% activation percentage of the nanoparticles in this range. This qualitatively suggests that the carbon-feeding effect is one of the most important mechanisms in determining the activation of nanoparticles in CVD growth of nanotubes. Further increases of carbon feeding rate cause fewer particles to be activated since the small particles are poisoned and lower the growth efficiency. Eventually, the growth of SWNTs is completely stopped by extensive particle poisoning due to excessive carbon feeding. It is believed that the reason for the low growth efficiency in many CVD processes is due to the mismatch of the growth conditions and the size distribution of the catalysts. This also points out the importance of controlling diameter distribution of nanoparticles for CVD growth of SWNTs with uniform diameters.

Interestingly, at the lower limits of effective growth range (4200 ppm for 800 °C and 140 ppm for 900 °C), the diameters of SWNTs are unexpectedly uniform, with standard deviations of 24% for 800 °C and 20% for 900 °C. Additionally, it is obvious that the diameter of nanotubes grown at 800 °C is smaller than those grown at 900 °C at the lower threshold of the effective growth window. This is because, at lower temperature, the activity of larger particles is further reduced, which results in the domination of thinner SWNTs. These results suggest a convenient way of producing thin SWNTs with very narrow diameter distribution, which may find its applications in hydrogen storage[14] and other application where small diameter nanotubes are desired.

In conclusion, the effect of carbon feeding rate on the diameter distribution of CVD-grown SWNTs was studied. It was found that diameters of SWNTs were closely related to the carbon feeding rate by selective activation of nanoparticles. Understanding the important role of the carbon feeding rate can be used to explain the cause of the low growth efficiency in most CVD processes and help us to design methods to improve the growth efficiency of the CVD growth of nanotubes. To achieve more efficient growth of uniform nanotubes, not only do the starting nanoparticles need to be uniform but also the carbon feeding rate needs to match the optimized growth conditions for such size of catalysts. It further reveals the importance of control on diameter distribution of nanoparticles for CVD growth of SWNTs with uniform diameters, since only nanoparticles with sizes close to an optimized size would grow SWNTs efficiently. Meanwhile, it shows the necessity of tuning the feeding gas composition to achieve the highest efficiency for any given set of nanoparticles.

Acknowledgment. The work is supported by a grant from DOE (DE-FC36-05GO15103) as part of the Center of Excellence for Carbon-Based Hydrogen Storage.

Supporting Information Available: Raman spectroscopy and growth efficiency of SWNTs. This material is available free of charge via the Internet at http://pubs.acs.org.

References and Notes

(1) Dai, H. J.; Rinzler, A. G.; Nikolaev, P.; Thess, A.; Colbert, D. T.; Smalley, R. E. *Chem. Phys. Lett.* **1996**, *260*, 471.
(2) Kong, J.; Cassell, A. M.; Dai, H. J. *Chem. Phys. Lett.* **1998**, *292*, 567.
(3) Hafner, J. H.; Bronikowski, M. J.; Azamian, B. R.; Nikolaev, P.; Rinzler, A. G.; Colbert, D. T.; Smith, K. A.; Smalley, R. E. *Chem. Phys. Lett.* **1998**, *296*, 195.
(4) Su, M.; Zheng, B.; Liu, J. *Chem. Phys. Lett.* **2000**, *322*, 321.
(5) Kong, J.; Soh, H. T.; Cassell, A. M.; Quate, C. F.; Dai, H. J. *Nature* **1998**, *395*, 878.
(6) Hata, K.; Futaba, D. N.; Mizuno, K.; Namai, T.; Yumura, M.; Iijima, S. *Science* **2004**, *306*, 1362.
(7) Li, Y. M.; Kim, W.; Zhang, Y. G.; Rolandi, M.; Wang, D. W.; Dai, H. J. *J. Phys. Chem. B* **2001**, *105*, 11424.
(8) Huang, S. M.; Woodson, M.; Smalley, R.; Liu, J. *Nano Lett.* **2004**, *4*, 1025.
(9) Franklin, N. R.; Dai, H. J. *Adv. Mater.* **2000**, *12*, 890.
(10) Zhang, Y.; Li, Y.; Kim, W.; Wang, D.; Dai, H. *Appl. Phys. A: Mater. Sci. Process.* **2002**, *74*, 325.
(11) He, M. S.; Duan, X. J.; Wang, X.; Zhang, J.; Liu, Z. F.; Robinson, C. *J. Phys. Chem. B* **2004**, *108*, 12665.
(12) Hornyak, G. L.; Grigorian, L.; Dillon, A. C.; Parilla, P. A.; Jones, K. M.; Heben, M. J. *J. Phys. Chem. B* **2002**, *106*, 2821.
(13) Wagg, L. M.; Hornyak, G. L.; Grigorian, L.; Dillon, A. C.; Jones, K. M.; Blackburn, J.; Parilla, P. A.; Heben, M. J. *J. Phys. Chem. B* **2005**, *109*, 10435.
(14) Cheng, H. S.; Cooper, A. C.; Pez, G. P.; Kostov, M. K.; Piotrowski, P.; Stuart, S. J. *J. Phys. Chem. B* **2005**, *109*, 3780.
(15) Choi, H. C.; Kim, W.; Wang, D. W.; Dai, H. J. *J. Phys. Chem. B* **2002**, *106*, 12361.
(16) Jeong, G. H.; Yamazaki, A.; Suzuki, S.; Yoshimura, H.; Kobayashi, Y.; Homma, Y. *J. Am. Chem. Soc.* **2005**, *127*, 8238.
(17) Han, S. J.; Yu, T. K.; Park, J.; Koo, B.; Joo, J.; Hyeon, T.; Hong, S.; Im, J. *J. Phys. Chem. B* **2004**, *108*, 8091.
(18) Jeong, H. J.; An, K. H.; Lim, S. C.; Park, M. S.; Chang, J. S.; Park, S. E.; Eum, S. J.; Yang, C. W.; Park, C. Y.; Lee, Y. H. *Chem. Phys. Lett.* **2003**, *380*, 263.
(19) Fu, Q.; Huang, S. M.; Liu, J. *J. Phys. Chem. B* **2004**, *108*, 6124.
(20) Cheung, C. L.; Kurtz, A.; Park, H.; Lieber, C. M. *J. Phys. Chem. B* **2002**, *106*, 2429.
(21) Javey, A.; Dai, H. J. *J. Am. Chem. Soc.* **2005**, *127*, 11942.
(22) An, L.; Owens, J. M.; McNeil, L. E.; Liu, J. *J. Am. Chem. Soc.* **2002**, *124*, 13688.
(23) Bachilo, S. M.; Balzano, L.; Herrera, J. E.; Pompeo, F.; Resasco, D. E.; Weisman, R. B. *J. Am. Chem. Soc.* **2003**, *125*, 11186.
(24) Miyauchi, Y. H.; Chiashi, S. H.; Murakami, Y.; Hayashida, Y.; Maruyama, S. *Chem. Phys. Lett.* **2004**, *387*, 198.
(25) Javey, A.; Shim, M.; Dai, H. J. *Appl. Phys. Lett.* **2002**, *80*, 1064.
(26) Alvarez, W. E.; Pompeo, F.; Herrera, J. E.; Balzano, L.; Resasco, D. E. *Chem. Mater.* **2002**, *14*, 1853.
(27) Harutyunyan, A. R.; Pradhan, B. K.; Kim, U. J.; Chen, G. G.; Eklund, P. C. *Nano Lett.* **2002**, *2*, 525.
(28) Paillet, M.; Jourdain, V.; Poncharal, P.; Sauvajol, J. L.; Zahab, A.; Meyer, J. C.; Roth, S.; Cordente, N.; Amiens, C.; Chaudret, B. *J. Phys. Chem. B* **2004**, *108*, 17112.
(29) Zhang, G. Y.; Mann, D.; Zhang, L.; Javey, A.; Li, Y. M.; Yenilmez, E.; Wang, Q.; McVittie, J. P.; Nishi, Y.; Gibbons, J.; Dai, H. J. *Proc. Natl. Acad. Sci. U.S.A.* **2005**, *102*, 16141.
(30) Endo, M.; Muramatsu, H.; Hayashi, T.; Kim, Y. A.; Terrones, M.; Dresselhaus, N. S. *Nature* **2005**, *433*, 476.
(31) Endo, M.; Hayashi, T.; Muramatsu, H.; Kim, Y. A.; Terrones, H.; Terrones, M.; Dresselhaus, M. S. *Nano Lett.* **2004**, *4*, 1451.